Magnetic Materials

DOI: 10.1002/ange.200805178

A Nanoscale Molecular Switch Triggered by Thermal, Light, and Guest Perturbation**

*Martin B. Duriska, Suzanne M. Neville, Boujemaa Moubaraki, John D. Cashion, Gregory J. Halder, Karena W. Chapman, Chérif Balde, Jean-François Létard, Keith S. Murray, Cameron J. Kepert, and Stuart R. Batten**

Molecule-based magnetic materials, such as those that display magnetic ordering or spin crossover (SCO), are attractive candidates for components in the data storage and electronics industries.[1] Miniaturization of next-generation advanced magnetic materials to the nanometer scale is required for their anticipated incorporation into electronic devices. While the application of supramolecular self-assembly (that is, the "bottom-up" approach) has been used to great effect in the production of large single molecular magnets,[2] recent efforts to produce nanoscale spin-switching systems have been focused on "top-down" approaches and alternative methods to the "bottom-up" approach, such as nanoparticle growth.[3]

It has also been realized that advanced, multifunctional magnetic materials may be generated through the incorporation of SCO properties into materials that have, for example, nanoporous natures.[4–6] In particular, it has been shown that guest removal and/or exchange in nanoporous polymeric framework materials can lead to remarkable changes in SCO behavior such that magnetism-based molecular sensing materials can be attained.

Herein we report the assembly, by using a "bottom-up" approach, of a nanoscale molecular metal–organic discrete switching nanoball, which shows a magnetic response to a range of external stimuli, including temperature, light, and solvent molecules. Of particular interest is its potential application as a light-sensitive magnetic device in which an "on" or "off" magnetic state can be readily selected by wavelength variation. This work also highlights the scope for manipulating the electronic state of discrete nanometer-sized inorganic molecules through solid-state guest exchange and removal.

The approach used to construct the metal–organic nanoball is outlined in Figure 1. The organic ligand employed, [tris{3-(4'-pyridyl)-pyrazol-1-yl}hydroborate] ($(Tp^{4-py})^-$) contains primary and secondary binding sites that are targeted in two distinct steps (Figure 1a). Firstly, the central tris(pyrazolyl)hydroborate core is utilized in an in situ, preorganizational step to form the neutral metalloligand $[Cu^I(Tp^{4-py})(CH_3CN)]$ (Figure 1b). This building block conformationally stabilizes

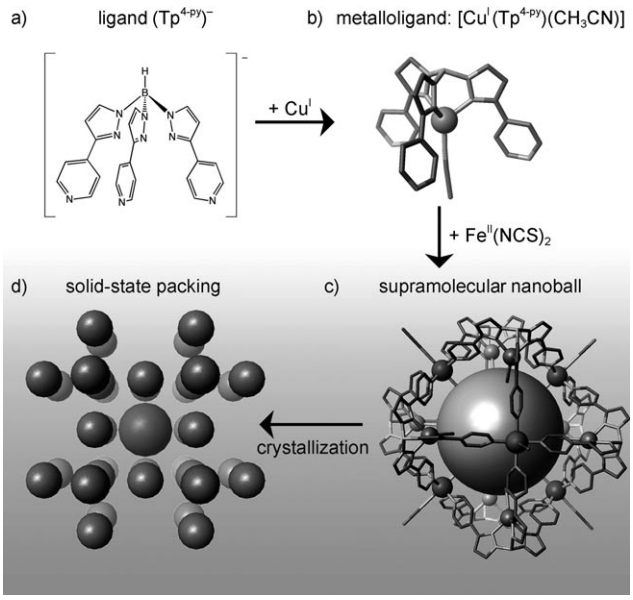

Figure 1. a) The bifunctional ligand, $[Tp^{4-py}]^-$ is used to form b) the rigid building block $[Cu^I(Tp^{4-py})(CH_3CN)]$. When Fe^{II} ions (and a thiocyanate salt) are added c) the supramolecular nanoball forms (the sphere is included to highlight the nanoball shape), which d) crystallize to form large pores of 3.5 nm diameter (larger central sphere).

[*] Dr. M. B. Duriska, Dr. S. M. Neville, Dr. B. Moubaraki, Prof. K. S. Murray, Assoc. Prof. S. R. Batten
School of Chemistry, Monash University, Vic 3800 (Australia)
Fax: (+61) 3-9905-4597
E-mail: stuart.batten@sci.monash.edu.au
Assoc. Prof J. D. Cashion
School of Physics, Monash University (Australia)
Dr. G. J. Halder
Materials Science Division, Argonne National Laboratory (USA)
Dr. K. W. Chapman
X-ray Science Division, Argonne National Laboratory (USA)
C. Balde, Dr. J.-F. Létard
Laboratoire des Sciences Moléculaires
ICMCB (CNRS UPR 9048) (France)
Prof. C. J. Kepert
School of Chemistry, University of Sydney (Australia)

[**] We thank the Australian Research Council, the protein crystallography beamline staff at the Australian Synchrotron, the Advanced Photon Source supported by the Australian Synchrotron Research Program, funded by the Commonwealth of Australia under the Major National Research Facilities Program, the National Science Foundation/Department of Energy (HE9522232 and CHE0087817) and the Illinois Board of Higher Education, the Argonne National Laboratory supported by the US Department of Energy, Basic Energy Sciences, Office of Science (DE-AC02-06CH11357), the French–Australia FAST/DEST grant, the Aquitaine Region, and Dr. Simon Iremonger for his assistance.

Supporting information for this article is available on the WWW under http://dx.doi.org/10.1002/anie.200805178.

an otherwise flexible organic ligand and directs the secondary binding sites (that is, the peripheral 4-pyridyl groups) for further reaction with an octahedral metal ion. In the second step, crystallization of the discrete nanoball species $[\{Cu^{I}(Tp^{4\text{-}py})(CH_3CN)\}_8\{Fe^{II}(NCS)_2\}_{10/3}\{Fe^{II}(NCS)(CH_3CN)\}_{8/3}]\cdot(ClO_4)_{8/3}\cdot(CH_3CN)_n$ occurs by self-assembly upon addition of Fe^{II} ions (and a thiocyanate salt; Figure 1c). This efficient one-pot, two-step synthesis affords near-quantitative yields of yellow cube-shaped crystals of the nanoball within 24 hours. Initial complexation with Cu^{I} ions to form the rigid, preorganized metalloligand appears to greatly favor its self-assembly and, furthermore, provides an added chemical functionality, that is, through possible variation of the metal and/or replacement of the bound solvent in the interior of the sphere. Overall, this two-step synthetic process provides a distinct contrast to other reported $[M_6L_8]^{n+}$-type supramolecular cages, which commonly utilize purely organic three-connecting ligands.[7]

Structural investigation of the individual nanoball species revealed a rigid $[Fe^{II}_6\{Cu^{I}(Tp^{4-py})\}_8]$ shell with an approximate diameter of 3 nm in which the octahedral arrangement of Fe^{II} ions and cubic arrangement of Cu^{I} ions forms a distorted rhombic dodecahedron.[8] In contrast to other similar discrete species,[9] the nanoballs pack inefficiently in the crystal lattice to form solvent-filled interstitial cuboctahedral cavities with an approximate diameter of 3.5 nm that account for about 30% of the crystal volume (Figure 1d).[10] While guest-accessible volumes in excess of 90% have been achieved in framework materials,[11] reports of porosity in metallo-supramolecular cages, other than the internal cage volume, are very uncommon.

Our motivation for the use of Fe^{II} ions to link $[Cu^{I}(Tp^{4-py})(CH_3CN)]$ units derives from the known potential magnetic switching capability of the $[Fe^{II}N_6]$ coordination environment.[12] Structurally, the nanoball incorporates $[Fe^{II}(NCS)_2(py)_4]$ (Fe-A) and $[Fe^{II}(NCS)(CH_3CN)(py)_4]$ (Fe-B) coordination environments (py refers to the $[Tp^{4-py}]$ coordination sites) in an approximate distribution of 56:44.[13] Each nanoball is thus cationic and the charge is balanced by clusters of perchlorate ions that lie in cavities created by their packing (which is different from the aforementioned solvent-filled regions, see the Supporting Information). While the Fe-A environment is most typically associated with SCO, the less well studied Fe-B environment can also be conducive to spin transitions.[14] Magnetic susceptibility studies over the temperature range 250–4 K reveal a spin transition of about 50% of the total Fe^{II} sites per nanoball from high spin (HS) to low spin (LS), such that the $\chi_M T$ values between 200 and 80 K decrease from 3.4 to 1.8 $cm^3 mol^{-1} K$ (Figure 2a). Below 10 K, the $\chi_M T$ values decrease more rapidly because of zero field splitting of the HS states. We note that the largest discrete systems that exhibit SCO thus far are the Fe_4^{II} grids reported by Lehn and co-workers,[15] which are significantly smaller than the nanoball presented here.

To identify which of the Fe^{II} environments switch magnetically, Mössbauer spectroscopy measurements were undertaken at 4.2 K, (see inset in Figure 4a) which reveal three distinct quadrupole doublets (LS: $\delta = 0.45\ mm\,s^{-1}$; $\Delta E_Q = 0.20\ mm\,s^{-1}$, area = 43%; HS $\delta = 1.19\ mm\,s^{-1}$; $\Delta E_Q = 1.37\ mm\,s^{-1}$, area = 36% and $\delta = 1.30\ mm\,s^{-1}$; $\Delta E_Q = 2.5\ mm\,s^{-1}$, area = 21%) comprising two HS sites (57%) and one LS site (43%).There are two crystallographically distinct Fe-A environments and a single Fe-B environment, which suggests that it is the latter rather than the former that is involved in the spin transition. This may be reasonably expected as acetonitrile has a stronger ligand field than thiocyanate.[14]

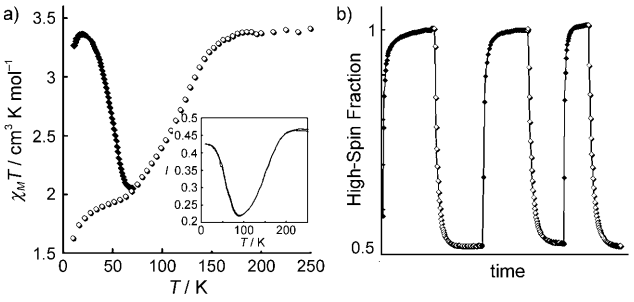

Figure 2. a) Plot of $\chi_M T$ versus temperature per Fe^{II} ion (○) and the light-induced excited metastable HS state with subsequent thermal relaxation (◆). The inset shows a plot of optical reflectivity signal versus temperature ($\lambda = 830$ nm) in the presence of white light. b) Cycling of the green- (◆) and red- (◇) light-induced switching between "on" (HS) and "off" (LS).

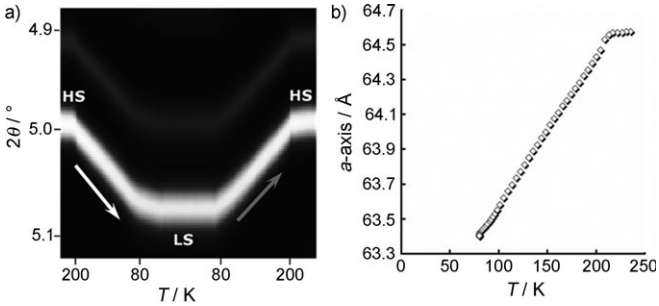

Figure 3. a) Powder X-ray diffraction peak position evolution (240–80–240 K). b) Plot of lattice parameter evolution versus temperature (240–80 K).

The structural consequence of electronic switching was followed by refining the cubic lattice parameter from synchrotron-based powder X-ray diffraction data over the temperature range 240→80→240 K. Qualitative examination of the patterns indicated a near-linear contraction and subsequent expansion of the cubic lattice over the temperature cycle (Figure 3a). The refined lattice parameters revealed an expansion of about 5.3% in lattice volume over this range (1.7% linear change; Figure 3b), which is attributed predominantly to geometric changes to the Fe-B coordination environment with crossover from LS to HS (that is, involving depopulation of t_{2g} orbitals and population of e_g orbitals with transformation from the $^1A_1$ ground state to $^5T_2$).

Beyond thermal switching, the nanoball undergoes light-induced switching by the light-induced excited spin state trapping (LIESST) effect. Photomagnetic measurements, undertaken by using SQUID magnetometry coupled with a green argon/krypton laser ($\lambda = 514.5$ nm) at 10 K, revealed a

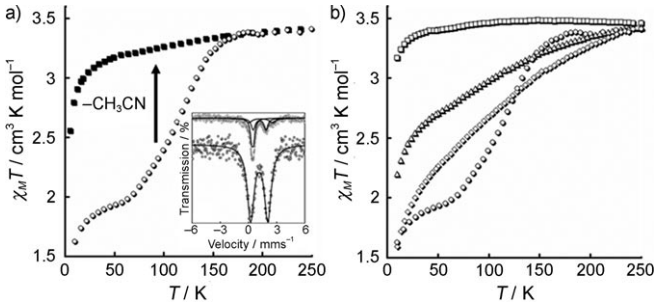

Figure 4. a) Plot of $\chi_M T$ versus T per Fe^{II} ion for the CH_3CN-sorbed (○) and desorbed species (●). The inset shows Mössbauer spectra (4 K) of the sorbed (top) and desorbed (bottom) materials. b) Plot of $\chi_M T$ versus temperature per Fe^{II} ion for sorbed solvents: CH_3CN (○), acetone (□), ethanol (△), and methanol (◇).

rapid increase in the magnetic signal from 1.6 to 3.4 $cm^3 mol^{-1} K$; this result was indicative of complete photoexcitation of the LS species to a "metastable" HS state (Figure 2a). This photoinduced "stored" information can be subsequently "erased" upon heating to approximately 55 K, or through irradiation using a red diode laser ($\lambda = 830$ nm) at 10 K by the reverse-LIESST effect. Repetitive cycling of the switching "on" (metastable HS state, "stored") and "off" (LS state, "erased") of the LIESST effect shows a completely reversible process that does not diminish with cycling (Figure 2b). Complementary temperature-dependent (10→270→10 K) and wavelength-dependent (450–950 nm) optical reflectivity measurements under white light showed changes in the d–d* (830 nm) and metal–ligand charge-transfer (550 nm) bands, which is consistent with the magnetic susceptibility of both the temperature and light-induced spin transition. In particular, between 270 and 70 K there is a decrease in the 830 nm band associated with the thermal spin transition, followed by an increase in this band between 70 and 10 K indicative of LIESST activity (see inset in Figure 2a).

The existence of large guest-filled cavities in the lattice between the nanoballs provides a further means to influence the SCO behavior through harnessing the interplay between guest inclusion and electronic groundstate.[4,5] Thermogravimetric analyses showed that the guest molecules located in the interstitial voids are removed upon heating to 75 °C, and that acetonitrile, methanol, ethanol, and acetone guests can be introduced both quantitatively and reversibly. Magnetic susceptibility data collected for a desorbed sample revealed a complete loss of SCO behavior, a common observance in nanoporous SCO systems (Figure 4a).[4] Mössbauer spectroscopy data collected at 4.2 K on this desorbed sample show a single quadrupole doublet ($\delta = 1.15$ mm s^{-1}; $\Delta E_Q = 1.82$ mm s^{-1}, area = 100 %), which is consistent with all HS Fe^{II} sites (see inset in Figure 4a). Upon immersion of the desorbed sample in acetonitrile, the SCO character of the sample returned and was found to be indistinguishable in behavior to that of the as-synthesized material. The guest-dependent SCO properties were further examined for samples where the acetonitrile guest molecules had been exchanged with methanol, ethanol, and acetone. The magnetic behaviors vary predominantly through a broadening of the spin transition over this series, with a complete loss of SCO being observed in the acetone-sorbed phase (Figure 4b).

In summary, this new molecular material—the switching nanoball—shows temperature-, light-, and guest-induced magnetic switching properties hitherto unexplored for large discrete metallo-supramolecular systems. The reversible light-induced switching between HS and LS states provides a possible path for selectively switching individual molecules "on" and "off". These 3 nm molecules could potentially, for example, be coated monodisperse on a solid surface in a display device or electronic switch. We also envisage the further adaptability of this highly versatile discrete system to a wide range of other industrially and environmentally important functions, such as gas storage and catalysis.

Experimental Section

A solution of [Cu^I(Tp^{4-py})(CH$_3$CN)] was prepared by adding Cu^I(ClO$_4$)·4 CH$_3$CN (15 mg, 0.05 mmol) to a solution of [TlTp^{4-py}] (30 mg, 0.05 mmol)[16] in CH_2Cl_2/CH_3CN (1:1, 5 mL). The nanoball was then prepared by adding a solution of Fe(ClO$_4$)$_2$·6 H$_2$O (8.8 mg, 0.03 mmol) and NaNCS (5.6 mg, 0.06 mmol) in CH_3CN (2 mL) to the solution of [Cu^I(Tp^{4-py})(CH$_3$CN)]. The resulting bright yellow solution was immediately filtered and, after slow evaporation over a period of 24 h, yellow crystals were obtained (yield: 44 mg, 95 %). IR (attenuated total reflection): $\tilde{\nu} = 2251$(m), 2051(s), 1616(s), 1487(w), 1464(w), 1428(m), 1367(s), 1189(s), 1100(sh), 1048(m), 1016(sh), 841(m), 734(s) cm^{-1}.

Single-crystal X-ray diffraction data were collected on the high-throughput protein crystallography beamline (15.5 keV, 3BM-1, Australian Synchrotron). Powder X-ray diffraction measurements were carried out at the Advanced Photon Source (20.02 keV, 0.61915 Å, 12-BM). Magnetic susceptibility data were collected using a Quantum Design MPMS-5 SQUID magnetometer (1 T). Optical reflectivity measurements were collected using a custom-built set-up equipped with a SM240 spectrometer (Opton Laser International). Magnetic susceptibility data (light-induced) were collected using a MPMS-55 Quantum design SQUID magnetometer (2 T) with a Kr^+ laser coupled through an optical fiber. Mössbauer spectroscopy was carried out by using a conventional constant acceleration drive with a symmetrical sawtooth waveform at liquid nitrogen (77 K) and liquid helium (4.2 K) temperatures.

Received: October 22, 2008
Published online: December 23, 2008

Keywords: host–guest systems · magnetic properties · nanostructures · spin crossover · supramolecular chemistry

[1] O. Kahn, *Acc. Chem. Res.* **2000**, *33*, 647; O. Kahn, C. J. Martinez, *Science* **1998**, *279*, 44; L. Cambi, L. Szego, *Ber. Dtsch. Chem. Ges.* **1931**, *64*, 2591.

[2] R. Sessoli, H.-L. Tsai, A. R. Schake, S. Wang, J. B. Vincent, K. Folting, D. Gatteschi, G. Christou, D. N. Hendrickson, *J. Am. Chem. Soc.* **1993**, *115*, 1804; W. Wernsdorfer, N. Aliaga-Alcalde, D. N. Hendrickson, G. Christou, *Nature* **2002**, *416*, 406.

[3] I. Boldog, A. B. Gaspar, V. Martínez, P. Pardo-Ibañez, V. Ksenofontov, A. Bhattacharjee, P. Gütlich, J. A. Real, *Angew. Chem.* **2008**, *120*, 6533; *Angew. Chem. Int. Ed.* **2008**, *47*, 6433; G. Molnár, S. Cobo, J. A. Real, F. Carcenac, E. Daran, C. Vieu, A. Bousseksou, *Adv. Mater.* **2007**, *19*, 2163; F. Volatron, L. Catala, E. Rivière, A. Gloter, O. Stéphan, T. Mallah, *Inorg. Chem.* **2008**,

47, 6584; E. Coronado, J. R. Galán-Mascarós, M. Monrabal-Capilla, J. García-Martínez, P. Pardo-Ibáñez, *Adv. Mater.* **2007**, *19*, 1359; T. Forestier, S. Mornet, N. Daro, T. Nishihara, S.-I. Mouri, K. Tanaka, O. Fouché, E. Freyszc, J.-F. Létard, *Chem. Commun.* **2008**, 4327.

[4] G. J. Halder, C. J. Kepert, B. Moubaraki, K. S. Murray, J. D. Cashion, *Science* **2002**, *298*, 1762.

[5] O. Kahn, J. Larionova, J. V. Yakhmi, *Chem. Eur. J.* **1999**, *5*, 3443.

[6] V. Niel, A. L. Thompson, M. C. Muñoz, A. Galet, A. E. Goeta, J. A. Real, *Angew. Chem.* **2003**, *115*, 3890 – 3893; *Angew. Chem. Int. Ed.* **2003**, *42*, 3760.

[7] D. K. Chand, K. Biradha, M. Fujita, S. Sakamoto, K. Yamaguchi, *Chem. Commun.* **2002**, 2486; S. Hiraoka, K. Harano, M. Shiro, Y. Ozawa, N. Yasuda, K. Toriumi, M. Shionoya, *Angew. Chem.* **2006**, *118*, 6638; *Angew. Chem. Int. Ed.* **2006**, *45*, 6488; M. Hong, Y. Zhao, W. Su, R. Cao, M. Fujita, Z. Zhou, A. Chan, *J. Am. Chem. Soc.* **2000**, *122*, 4819; D. Moon, S. Kang, J. Park, K. Lee, R. P. John, H. Won, G. H. Seong, Y. S. Kim, G. H. Kim, H. Rhee, M. S. Lah, *J. Am. Chem. Soc.* **2006**, *128*, 3530; B. Moulton, J. Lu, A. Mondal, M. J. Zaworotko, *Chem. Commun.* **2001**, 863; T. K. Ronson, J. Fisher, L. P. Harding, M. J. Hardie, *Angew. Chem.* **2007**, *119*, 9244; *Angew. Chem. Int. Ed.* **2007**, *46*, 9086.

[8] Crystal data: $C_{716}H_{600}B_{24}Cl_8Cu_{24}Fe_{18}N_{300}O_{40}S_{28}$, $M_r = 18017.94$, cubic, $Fm\bar{3}c$, $T = 200$ K, $a = 63.445(7)$ Å, $V = 255380(50)$ Å^3, $Z = 8$, $\mu(Mo_{K\alpha}) = 0.700$ mm^{-1}. Data were collected using synchrotron radiation ($\lambda = 0.77314$ Å) at the Australian Synchrotron Facility by using a nitrogen gas cryostream. Full-matrix least squares refinements on F_o^2 converged to $R1 = 0.0832$, $wR2 = 0.2460$.

[9] H. Furukawa, J. Kim, N. Ockwig, M. O'Keefe, O. M. Yaghi, *J. Am. Chem. Soc.* **2008**, *130*, 11650; S. Ghosh, P. S. Mukherjee, *J. Org. Chem.* **2006**, *71*, 8412; R. W. Larsen, G. J. McManus, J. J. Perry, E. Rivera-Otero, M. J. Zaworotko, *Inorg. Chem.* **2007**, *46*, 5904; G. J. McManus, Z. Wang, M. J. Zaworotko, *Cryst. Growth Des.* **2004**, *4*, 11; M. Tominaga, K. Suzuki, T. Murase, M. Fujita, *J. Am. Chem. Soc.* **2005**, *127*, 11950.

[10] PLATON, A Multipurpose Crystallographic Tool, A L. Spek, Utrecht University, The Netherlands, **2000**.

[11] M. Eddaoudi, J. Kim, N. Rosi, D. Vodak, J. Wachter, M. O'Keeffe, O. M. Yaghi, *Science* **2002**, *295*, 469; S. S. Han, H. Furukawa, O. M. Yaghi, W. A. Goddard, *J. Am. Chem. Soc.* **2008**, *130*, 11580.

[12] P. Gütlich, H. A. Goodwin, *Top. Curr. Chem.* **2004**, *233*, 1.

[13] There are a total of six Fe^{II} sites in each nanoball, which are composed of two crystallographically distinct sites, Fe1 and Fe2. The two Fe1 sites have a $[Fe(NCS)_2(py)_4]$ (Fe-A) coordination environment, while the four Fe2 sites have a 1/3 occupancy of the Fe-A coordination environment and a 2/3 occupancy of the Fe-B environment. This equates to 2 (Fe1) + 4/3 (Fe2) of the Fe-A type sites per nanoball (that is, 56% of the total six Fe^{II} sites), with the remainder comprising Fe-B sites.

[14] H. Toftlund, J. J. McGarvey, *Top. Curr. Chem.* **2004**, *233*, 151.

[15] M. Ruben, E. Breuning, J. M. Lehn, V. Ksenofontov, F. Renz, P. Gütlich, G. B. M. Vaughan, *Chem. Eur. J.* **2003**, *9*, 4422.

[16] H. Adams, S. R. Batten, G. M. Davies, M. B. Duriska, J. C. Jeffery, P. Jensen, J. Lu, G. R. Motson, S. J. Coles, M. B. Hursthouse, M. D. Ward, *Dalton Trans.* **2005**, 1910.

